

7-2-2019

Oomycete Metabarcoding Reveals the Presence of Lagenidium spp. in Phytotelmata

Paula Leoro-Garzon

Nova Southeastern University

Andrew J. Gonedes

Nova Southeastern University

Isabel Olivera

Nova Southeastern University

Aurelien Tartar

Nova Southeastern University, aurelien@nova.edu

Follow this and additional works at: https://nsuworks.nova.edu/cnso_bio_facarticles

 Part of the [Biology Commons](#)

NSUWorks Citation

Leoro-Garzon, Paula; Andrew J. Gonedes; Isabel Olivera; and Aurelien Tartar. 2019. "Oomycete Metabarcoding Reveals the Presence of Lagenidium spp. in Phytotelmata." *PeerJ Preprints*, (): e27835v1. doi:10.7287/peerj.preprints.27835v1.

This Article is brought to you for free and open access by the Department of Biological Sciences at NSUWorks. It has been accepted for inclusion in Biology Faculty Articles by an authorized administrator of NSUWorks. For more information, please contact nsuworks@nova.edu.

Oomycete metabarcoding reveals the presence of *Lagenidium* spp. in phytotelmata

Paula Leoro-Garzon¹, Andrew J Gonedes¹, Isabel E Olivera¹, Aurelien Tartar^{Corresp. 1}

¹ Department of Biological Sciences, Nova Southeastern University, Fort Lauderdale, FL, United States

Corresponding Author: Aurelien Tartar
Email address: aurelien@nova.edu

The oomycete genus *Lagenidium*, which includes the mosquito biocontrol agent *L. giganteum*, is composed of animal pathogens, yet is phylogenetically closely related to the well characterized plant pathogens *Phytophthora* and *Pythium* spp. These phylogenetic affinities were further supported by the identification of canonical oomycete effectors in the *L. giganteum* transcriptome, and suggested, mirroring the endophytic abilities demonstrated in entomopathogenic fungi, that *L. giganteum* may have similarly retained capacities to establish interactions with plant tissues. To test this hypothesis, culture-independent, metabarcoding analyses aimed at detecting *L. giganteum* in bromeliad phytotelmata (a proven mosquito breeding ground) microbiomes were performed. Two independent and complementary microbial detection strategies based on the amplification of *cox1* DNA barcodes were used and produced globally concordant outcomes revealing that two distinct *Lagenidium* phylotypes are present in phytotelmata. A total of 23,869 high quality reads were generated from four phytotelmata, with 52%, and 11.5%, corresponding to oomycetes, and *Lagenidium* spp., barcodes, respectively. Newly-designed *Lagenidium*-specific *cox1* primers combined with cloning/Sanger sequencing produced only *Lagenidium* spp. barcodes, with a majority of sequences clustering with *L. giganteum*. High throughput sequencing based on a Single Molecule Real Time (SMRT) approach combined with broad range *cox1* oomycete primers confirmed the presence of *L. giganteum* in phytotelmata, but indicated that a potentially novel *Lagenidium* phylotype (closely related to *L. humanum*) may represent one of the most prevalent oomycetes in these environments (along with *Pythium* spp.). Phylogenetic analyses demonstrated that all detected *Lagenidium* phylotype *cox1* sequences clustered in a strongly-supported, monophyletic clade that included both *L. giganteum* and *L. humanum*. Therefore, *Lagenidium* spp. are present in phytotelmata microbiomes. This observation provides a basis to investigate potential relationships between *Lagenidium* spp. and phytotelma-forming plants, especially in the absence of water and/or invertebrate hosts, and reveals phytotelmata as sources for the identification of novel *Lagenidium* isolates with potential

as biocontrol agents against vector mosquitoes.

1
2
3
4
5
6
7
8
9
10
11
12
13
14
15
16
17
18
19
20
21
22
23
24
25
26
27
28

**Oomycete metabarcoding reveals the presence of
Lagenidium spp. in phytotelmata**

Paula Leoro-Garzon, Andrew J. Gonedes, Isabel E. Olivera, Aurelien Tartar*

Department of Biological Sciences, Nova Southeastern University, Fort Lauderdale, FL, USA

* Author for correspondence: 3301 College Avenue, Fort Lauderdale, FL 33314, USA. Phone: 9542628148, Fax: 9542624240, Email: aurelien@nova.edu

29 **ABSTRACT**

30 The oomycete genus *Lagenidium*, which includes the mosquito biocontrol agent *L. giganteum*, is
31 composed of animal pathogens, yet is phylogenetically closely related to the well characterized
32 plant pathogens *Phytophthora* and *Pythium* spp. These phylogenetic affinities were further
33 supported by the identification of canonical oomycete effectors in the *L. giganteum*
34 transcriptome, and suggested, mirroring the endophytic abilities demonstrated in
35 entomopathogenic fungi, that *L. giganteum* may have similarly retained capacities to establish
36 interactions with plant tissues. To test this hypothesis, culture-independent, metabarcoding
37 analyses aimed at detecting *L. giganteum* in bromeliad phytotelmata (a proven mosquito
38 breeding ground) microbiomes were performed. Two independent and complementary microbial
39 detection strategies based on the amplification of *cox1* DNA barcodes were used and produced
40 globally concordant outcomes revealing that two distinct *Lagenidium* phylotypes are present in
41 phytotelmata. A total of 23,869 high quality reads were generated from four phytotelmata, with
42 52%, and 11.5%, corresponding to oomycetes, and *Lagenidium* spp., barcodes, respectively.
43 Newly-designed *Lagenidium*-specific *cox1* primers combined with cloning/Sanger sequencing
44 produced only *Lagenidium* spp. barcodes, with a majority of sequences clustering with *L.*
45 *giganteum*. High throughput sequencing based on a Single Molecule Real Time (SMRT)
46 approach combined with broad range *cox1* oomycete primers confirmed the presence of *L.*
47 *giganteum* in phytotelmata, but indicated that a potentially novel *Lagenidium* phylotype (closely
48 related to *L. humanum*) may represent one of the most prevalent oomycetes in these
49 environments (along with *Pythium* spp.). Phylogenetic analyses demonstrated that all detected
50 *Lagenidium* phylotype *cox1* sequences clustered in a strongly-supported, monophyletic clade that
51 included both *L. giganteum* and *L. humanum*. Therefore, *Lagenidium* spp. are present in

52 phytotelmata microbiomes. This observation provides a basis to investigate potential
53 relationships between *Lagenidium* spp. and phytotelma-forming plants, especially in the absence
54 of water and/or invertebrate hosts, and reveals phytotelmata as sources for the identification of
55 novel *Lagenidium* isolates with potential as biocontrol agents against vector mosquitoes.

56

57

58 **INTRODUCTION**

59

60 Oomycetes are heterotrophic eukaryotes that are morphologically similar to fungi but
61 phylogenetically related to diatoms and brown algae, and grouped with these photosynthetic
62 relatives within the phylum Heterokonta (Derevnina et al. 2016; Kamoun et al. 2015). The best-
63 characterized oomycetes are disease-causing agents with significant impacts on human activities
64 and food security, and the majority of the work directed at understanding the biology of
65 oomycetes is aimed at controlling or eliminating these organisms from anthropogenic
66 agroecosystems such as crop fields or aquaculture facilities (Derevnina et al. 2016). A minority
67 of oomycetes have potential as biological control agents, including the mycoparasite *Pythium*
68 *oligandrum* (Horner et al. 2012) and the mosquito pathogen *Lagenidium giganteum* (Kerwin et
69 al. 1994), and have been developed as the commercial products Polyversum and Laginex,
70 respectively. However, safety concerns over the true host range of *L. giganteum* (Vilela et al.
71 2015) have prompted a shift from large-scale production and commercialization to molecular
72 explorations directed at identifying bioactive compounds that may be translated into novel
73 mosquito control strategies (Singh & Prakash 2010). The recent transcriptome analyses of *L.*
74 *giganteum* have also contributed in expanding the characterization of oomycete diversity at the
75 molecular level (Olivera et al. 2016; Quiroz Velasquez et al. 2014). Sequence analyses suggested
76 that *L. giganteum* evolved from plant pathogenic ancestors and has retained genes typically
77 associated with plant tissues infections, such as the CRN or CBEL effectors that have been
78 extensively characterized in *Phytophthora infestans* and related plant pathogenic species. In
79 addition, the *L. giganteum* transcriptome was shown to contain several genes that were absent
80 from plant pathogenic genomes, and that were conserved either in entomopathogenic eukaryotes

81 (Quiroz Velasquez et al. 2014), or in animal pathogenic oomycetes (Olivera et al. 2016).
82 Specifically, carbohydrate-active GH5_27 and GH20 genes were found to be up-regulated in the
83 presence of insect hosts, and were predicted to exhibit biological activities against insect-specific
84 substrates (Olivera et al. 2016).

85 The emerging dichotomy reflected by the *L. giganteum* transcriptome is reminiscent of the most
86 recent analyses of fungal entomopathogens genomes, and suggests that similarities between
87 fungal and oomycetes entomopathogens may be extended from morphology and pathological
88 strategies to evolutionary history and ecological relationships. Genomic analyses have
89 demonstrated that two of the most common genera of insect-pathogenic fungi, *Metarhizium* and
90 *Beauveria*, have evolved from plant pathogens, and have retained genes indicative of plant
91 interactions (Moonjely et al. 2016; Wang et al. 2016). In fact, both *Metarhizium* and *Beauveria*
92 spp. are now widely regarded as plant endophytes that maintain significant symbiotic
93 relationships with their plant hosts, where insect infections, and subsequent nitrogen transfer
94 from insect to plant tissues (Behie & Bidochka 2014), may play only a small role among the
95 diverse beneficial interactions that have been shown to result from the presence of these fungi in
96 plants and their rhizospheres (Lopez & Sword 2015; Sasan & Bidochka 2012). In agreement
97 with these recent studies, the oomycete *L. giganteum* have been hypothesized as a potential
98 endophyte that can alternate between plant and insect hosts, and has the genomic resources to
99 engage in both type of relationships (Quiroz Velasquez et al. 2014). Most *Lagenidium* spp.
100 isolations have followed episodic observations of colonization in various animal host tissues
101 (Mendoza et al. 2016; Nakamura et al. 1995; Vilela et al. 2019), and therefore, to date, there is
102 little evidence of meaningful ecological associations between *Lagenidium* spp. and plants.
103 However, phytotelmata appear as likely habitats for *Lagenidium* spp, based on a previous study

104 that reported *Lagenidium*-infected invertebrates in plant axils (Frances et al. 1989), and on the
105 well-established knowledge that phytotelmata represent ideal breeding grounds for *L. giganteum*
106 potential hosts, including mosquitoes (Derraik 2009). The role of phytotelmata as mosquito
107 breeding sites has been recently highlighted by South Florida-based studies indicating that *Aedes*
108 *aegypti* mosquitoes (the main vectors for dengue fever, yellow fever and zika) may successfully
109 evade vector control strategies by breeding in popular and difficult-to-treat ornamental
110 bromeliads (Wilke et al. 2018).

111 To test the hypothesis that *Lagenidium giganteum* inhabit phytotelmata (especially, South
112 Florida bromeliad phytotelmata) and therefore may establish tripartite interactions with both
113 insect and plant hosts, a culture-independent assay aimed at detecting *Lagenidium* spp. barcodes
114 (metabarcoding) was developed. Molecular-based approaches based on the PCR amplification of
115 selected DNA barcodes have been used for multiple phyla and multiple environments, and a
116 wealth of information have been compiled in databases such as the Barcode Of Life Data system
117 (Ratnasingham & Hebert 2007). Standard barcodes consist of *cox1* and ITS gene regions for
118 animals and fungi, respectively, whereas plant barcoding has relied on multiple chloroplastic
119 markers (Adamowicz 2015). A barcode consensus for oomycetes has yet to emerge. Previous
120 studies have proposed and tested several potential candidate genes, including the ITS region (Riit
121 et al. 2016; Robideau et al. 2011), and the *cox1*, *cox2*, and cytochrome *b* genes (Choi et al. 2015;
122 Giresse et al. 2010; Robideau et al. 2011). Most of these oomycete barcoding efforts have been
123 restricted to assessing phylum-specific primers on DNA preparations obtained from axenically-
124 grown isolates, and few have transitioned to primer validation assays that (i) incorporated
125 environmental sampling, and (ii) combined primers with specific sequencing
126 strategies/platforms. Pioneer oomycete metabarcoding studies have favored the use of ITS

127 primers, and the production of small size amplicons (Prigigallo et al. 2016; Riit et al. 2016;
128 Sapkota & Nicolaisen 2015). Oomycete metagenomics has yet to fully integrate third generation
129 sequencing technologies that enable long read analyses, despite recent studies demonstrating that
130 strategies such as the Single Molecule Real Time (SMRT) method developed by Pacific
131 Biosciences (known as PacBio sequencing) delivered similar barcoding sequencing
132 performances compared to other platforms while producing much longer (and therefore more
133 informative) DNA barcodes (Pootakham et al. 2017; Wagner et al. 2016). These improvements
134 in long read sequencing quality provide a renewed opportunity to assess the *coxI* gene as a
135 oomycete barcode, since oomycete-specific *coxI* primers have already been published, and they
136 produce the longest (>600bp) oomycete barcode evaluated to date (Choi et al. 2015). In light of
137 this new possibility, the purpose of this study was two-fold: first, to develop *Lagenidium*
138 *giganteum*-specific *coxI* primers to assess the presence of this entomopathogenic oomycete in
139 bromeliad phytotelmata, and second, to couple the use of previously published oomycete-
140 specific *coxI* primers with SMRT-based sequencing strategy, and assess the potential of this
141 combination to not only confirm the presence of *L. giganteum* in phytotelmata, but also evaluate
142 the relative abundance of *L. giganteum* among other phytotelmata-inhabiting oomycete species.
143

144 MATERIALS AND METHODS

145

146 **Oomycete cultures, *coxI* gene sequencing, and genus-specific primer design:** The
147 *Lagenidium giganteum* strain ARSEF 373 was accessed from the USDA Agricultural Research
148 Service Collection of Entomopathogenic Fungal Cultures (ARSEF, Ithaca, NY) and was grown
149 in a defined Peptone-Yeast-Glucose (PYG) media supplemented with 2mM CaCl₂, 2mM MgCl₂

150 and 1ml/L soybean oil (Kerwin & Petersen 1997). Axenic cultures were processed for genomic
151 DNA extraction using the Qiagen DNeasy minikit, as previously described (Olivera et al. 2016;
152 Quiroz Velasquez et al. 2014). The genomic DNA preparations were used as templates in
153 Polymerase Chain Reactions (PCR) in combination with the oomycete-specific *coxI* primers
154 OomCoxI-Levup (5'-TCAWCWMGATGGCTTTTTTCAAC-3') and OomCoxI-Levlo (5'-
155 CYTCHGGRTGWCCRAAAAACCAAA-3'). These primers were designed to overlap the
156 standard *coxI* DNA barcode used in other groups and recommended by the Consortium for the
157 Barcode of Life (CBOL) initiative (Robideau et al. 2011). PCR conditions corresponded to the
158 following pattern repeated for 30 cycles: 95 °C for 30 s, 50 °C for 30 s, and 72 °C for 1 min. The
159 resulting products were purified using the QIAquick PCR purification Kit (Qiagen, USA) and
160 sequenced commercially using traditional Sanger technology (Macrogen USA). The generated
161 sequences were aligned with homologous oomycete sequences obtained from the Barcode of
162 Life Data System (BOLD) database of *coxI* genes (Ratnasingham & Hebert 2007). Alignments
163 were performed using ClustalX with default parameters (Larkin et al. 2007). The *coxI* gene
164 alignment was used to visually identify regions suitable for genus- or species-specific primer
165 design. Alignments corresponding to selected locations were used as inputs for the construction
166 of sequence logos using WebLogo, version 3 (Crooks et al. 2004).

167 **Phytotelmata sampling and plant identification:** Phytotelmata were sampled from ornamental
168 plants on the Nova Southeastern University main campus in Fort Lauderdale, FL, USA. The
169 plants were selected based on two criteria, including a visual, tentative taxonomic
170 characterization of plants as bromeliads, and the observable presence of a large volume of water
171 within the plants axils. The precise location of each plant was recorded using the Global Position
172 System (GPS). Phytotelmata samples consisted of a 100 mL volume of water collected using

173 sterile serological pipettes, and transferred in sterile 50 mL conical tubes. The water samples
174 were inspected visually for the presence of macroscopic debris and invertebrates. In addition,
175 leaf tissues (2 to 3 cm²) were also sampled for each plant, in an effort to associate phytotelmata
176 samples with plant taxonomic classification. The leaf samples were grounded in liquid nitrogen
177 and processed for DNA extraction using the Qiagen DNeasy Plant Mini kit (according to the
178 manufacturer's instructions). The plant genomic DNA preparations were used to PCR-amplify
179 plant barcodes using primers designed for previously characterized loci, including the *trnH-psbA*
180 spacer region (Kress & Erickson 2007; Kress et al. 2005) and the internal transcribed spacer
181 (ITS) region of nuclear rDNA (Cheng et al. 2016) traditionally used for a wide variety of land
182 plants, as well as the *trnC-petN* spacer marker used more specifically for bromeliad barcoding
183 (Versieux et al. 2012).

184 **Phytotelmata microbiomes DNA extractions and *coxI* barcode amplification:** Phytotelmata
185 samples were vacuum-filtered through 47mm diameter, 0.45µm pore size nitrocellulose filters
186 (Millipore), as previously described (Mancera et al. 2012), and the microbial fauna retained on
187 these filters was subjected to DNA extraction using the MoBio PowerWater DNA isolation kit
188 (according to the manufacturer's instructions). A similar workflow (vacuum filtration and DNA
189 extraction) was used to process negative control water samples. These samples consisted of 100
190 mL of water collected at a drinking water fountain located on the NSU campus, as well as a 100
191 mL of seawater collected off the coast of Hollywood Beach, FL, USA. The resulting
192 metagenomic DNA preparations obtained from phytotelmata and negative controls samples were
193 initially PCR amplified using the oomycete-specific *coxI* primers OomCoxI-Levup and
194 OomCoxI-Levlo and the reaction parameters described above. Products of these PCR reactions
195 were visualized on agarose gels. Subsequently, aliquots (1µl, non purified) corresponding to the

196 products from the first round of amplification were used as templates for a second round of
197 amplification. These nested PCR reactions were performed using the *Lagenidium*-specific
198 primers under stringent conditions (30 cycles of the following pattern: 95 °C for 30 s, 68 °C for
199 30 s, and 72 °C for 1 min). Products of these PCR reactions were visualized on agarose gels,
200 cloned using the Invitrogen TOPO technology and processed for commercial Sanger sequencing
201 (Macrogen USA). Resulting sequences were evaluated through homology searches and
202 phylogenetic analyses as described below.

203 **Oomycete community assessment through *cox1* metabarcoding:** The phytotelmata *cox1*
204 libraries were prepared for single molecule real time (SMRT) sequencing using recommended
205 protocols available from Pacific Biosciences (PacBio multiplexed SMRTbell libraries). The
206 workflow included a two-step PCR amplification as previously published (Pootakham et al.
207 2017). First, fusion primers were custom designed by combining the OomCoxI-Levup and
208 OomCoxI-Levlo primer sequences described above with the PacBio universal sequence. These
209 primers were HPLC purified and further modified by the addition of a 5' block (5'-NH₄, C6) to
210 ensure that carry-over amplicons from the first round of PCR were not ligated in the final
211 libraries (Integrated DNA Technologies). The first PCR reaction used these primers to amplify
212 *cox1* fragments from all four phytotelmata metagenomic DNA preparations. Resulting products
213 were gel-extracted and served as templates for the second PCR reactions. The second reaction
214 used the PacBio Barcoded Universal Primers (BUP) so that unique combinations of
215 (symmetrical) forward and reverse barcoded primers were associated with each phytotelmata
216 samples. Products of the second amplification were purified (DCC, Zymo Research), and sent to
217 the University of Florida Interdisciplinary Core for Biotechnology Research (ICBR) where
218 amplicons were pooled in equimolar concentrations and further processed for library

219 construction and SMRT sequencing. The PacBio raw reads were demultiplexed and assessed for
220 quality at the ICBR. Quality control processing included eliminating poor quality sequences,
221 sequences outside the expected amplification size (ca. 810 bp) and sequences that failed to
222 include both flanking, symmetrical barcodes. High quality reads served as inputs for homology
223 searches to assign taxonomic identification down to the genus level, using BLAST2GO (Conesa
224 et al. 2005). Sequences homologous to *Lagenidium* spp. were further processed for thorough
225 phylogenetic analyses. These sequences were trimmed to eliminate flanking 5' and 3' regions,
226 and evaluated for redundancy (100% homology) and OTU clustering using the ElimDupes tool
227 (<http://www.hiv.lanl.gov/>). Selected sequences were included in the alignment described below.

228 **Phylogenetic analyses:** The *cox1* gene sequences generated from axenic cultures and
229 environmental samples were aligned with homologous oomycete sequences using ClustalX
230 (Larkin et al. 2007). Most orthologous sequences were downloaded from the BOLD database
231 (Ratnasingham & Hebert 2007) as described above. However, the alignment was also
232 complemented with orthologous *Lagenidium* spp. sequences available from GenBank, including
233 the *cox1* sequenced fragments recently generated from *Lagenidium* spp. isolates collected on
234 mammalian tissues (Spies et al. 2016). The complete *cox1* alignment consisted of a 620-
235 character dataset that contained 62 taxa. The position of the shorter, Sanger-based environmental
236 sequences was inspected visually and confirmed based on the location of the *Lagenidium*-
237 specific primers. The jModeltest program (Darriba et al. 2012) was used to identify the most
238 appropriate maximum likelihood (ML) base substitution model for this dataset. The best-fit
239 model consistently identified by all analyses was the Generalized Time Reversible model with a
240 gamma distribution for variable sites, and an inferred proportion of invariants sites (GTR+G+I).
241 ML analyses that incorporated the model and parameters calculated by jModeltest were

242 performed using PhyML3.0 (Guindon et al. 2010). ML bootstrap analyses were conducted using
243 the same model and parameters in 1,000 replicates. The phylogenetic tree corresponding to the
244 ML analyses was edited using FigTree v. 1.4.4.

245

246 RESULTS

247

248 ***Lagenidium giganteum* *cox1* gene sequence analysis:** The *cox1* fragment generated from the
249 *Lagenidium giganteum* strain ARSEF373 was 683 bp long, and its sequence was deposited in the
250 GenBank/EMBL/ DDBJ databases under the accession number MN099105. Homology searches
251 (not shown) demonstrated that the generated sequence was 100% identical to *cox1* sequences
252 reported from two other strains of *L. giganteum* (strains ATCC 52675, and CBS 58084, with
253 *cox1* sequences publicly accessible under the accession numbers KF923742 and HQ708210,
254 respectively). Both strains ARSEF 373 and ATCC 52675 were originally isolated from mosquito
255 larvae, according to culture collection records. Further comparisons (not shown) indicated that
256 sequences from these mosquito-originating strains appeared divergent from the *cox1* fragments
257 sequences generated from multiple strains of *L. giganteum* f. *caninum* that have been reported as
258 mammal pathogens, yet also retained the ability to infect mosquito in laboratory settings (Vilela
259 et al. 2015). These results highlight the potential of molecular barcodes such as *cox1* to
260 distinguish between the known *Lagenidium* strains.

261 Unsurprisingly, the entomopathogenic *L. giganteum* *cox1* sequences were also different from
262 sequences characterizing more phylogenetically-distant oomycetes, including *Lagenidium*,
263 *Pythium* and *Phytophthora* spp., as well as other Peronosporales. These differences provided a
264 basis to develop *Lagenidium giganteum*-specific primers, and the location ultimately selected for

265 primer design is illustrated in Figure 1. The specificity of the designed primers relied especially
266 on the reverse primer, that is located on a region that is immediately (40 bp) upstream the
267 OomCoxI-Levlo primer (Fig 1). This region was characterized by the presence of a 5'-ATCA-3'
268 motif that was showed to be prevalent in *Lagenidium*: alignments demonstrated that it was
269 present on all the publicly available *cox1* sequences (41 sequences total) obtained from *L.*
270 *giganteum* (both mosquito and mammal strains) as well as *L. humanum* (Fig. 1). In contrast, the
271 motif was not found in *L. deciduum* sequences (3 sequences), and was found only sporadically in
272 *Pythium* and *Phytophthora* sequences (most notably in *Py. helicandrum*, *Py. carolinianum*, and
273 some strains of *P. ramorum*, *P. cactorum* and *P. infestans*). As a result, the reverse *Lagenidium*-
274 specific primer was designed to incorporate the reverse complement sequence 5'-TGAT-3' at its
275 3' end, and overlapped additional polymorphic sequences between *Lagenidium* and other
276 Peronosporales. The primer sequences were finalized at 5'-ACTGGATCTCCTCCTCCTGAT-3'
277 for the reverse primer, and 5'-TAACGTGGTTGTAAGTGCAC-3' for the matching forward
278 primer.

279 **Environmental detection of *Lagenidium* spp. in phytotelmata using Sanger sequencing:** A
280 total of four plants were selected for analysis (Fig. 2). These plants were all characterized by a
281 leaf axil structure that allowed for the retention of sampleable volumes of water. Anecdotal
282 observations supported the hypothesis that invertebrates used these sources of water, as several
283 dead and live insects, including mosquito larvae and pupae, were readily pipetted during water
284 sampling (not shown). Taxonomic identification of these plants relied in part on the sequencing
285 of plant barcodes. Sequence fragments corresponding to the chloroplastic *trnH-psbA* and the
286 *trnC-petN* spacer regions were obtained for all plants. Sequences ranged from 163 to 597 bp, and
287 403 to 641 bp, for the *trnH-psbA* and the *trnC-petN* barcodes, respectively, and are available

288 publicly in the GenBank/EMBL/ DDBJ databases under the accession numbers MN099106-
289 MN099113. Homology searches (not shown) identified all plants as members of the family
290 Bromeliaceae, in agreement with tentative taxonomic classifications based on morphological
291 characteristics. Taxonomical identifications at the genus and species levels were not attempted.
292 The oomycete- and *Lagenidium*-specific *cox1* primers were used in combination with
293 metagenomic DNA preparations representative of the four plant phytotelmata (Fig. 2). As
294 illustrated in Figure 2, the first round of amplification, using oomycete- specific *cox1* primers,
295 consistently produced detectable amplicons of the expected size (ca. 700 bp) for all plant-based
296 water sources, but not the control water sources, strongly suggesting the presence of oomycetes
297 in the four sampled phytotelmata. Similarly, the nested PCR amplifications, using *Lagenidium*-
298 specific primers (Fig. 1) and stringent PCR conditions, also produced fragments of the expected,
299 525 bp- size (not shown). These fragments were cloned, and randomly-selected clones were
300 sequenced, leading to the production of twelve high-quality sequences (three per plants). The
301 sequences were all 484 bp long (primers excluded), and are available publicly in GenBank under
302 the accession numbers MN099114- MN099125. Homology searches demonstrated that all twelve
303 of these newly-obtained, environmental sequences were more similar to *Lagenidium* spp. *cox1*
304 sequences than other any oomycete barcodes (not shown). However, sequence alignments also
305 revealed that none of the environmental sequences were 100% identical to the previously
306 published *Lagenidium* spp. barcodes obtained from known strains maintained in axenic cultures
307 (based on the 484 bp fragment length), suggesting a yet-unsampled diversity within the
308 *Lagenidium* genus. Using a traditional 97% distance level to build Operational Taxonomic Unit
309 (OTUs), the twelve Sanger-based sequences clustered in two distinct OTUs. The first OTU
310 consisted of the *Lagenidium humanum cox1* barcode (accession number KC741445) clustered

311 with the three sequences obtained from P3 (these three sequences were identical) and two
312 identical sequences from the P1 phytotelma. All other environmental sequences (three identical
313 sequences from the P4 phytotelma, as well as one unique sequence from P1, and three unique
314 sequences from P2) clustered in a second OTU that included all known *cox1* sequences from *L.*
315 *giganteum*, including the *L. giganteum* f. *caninum* *cox1* barcodes. These preliminary findings
316 strongly suggested that all environmental sequences corresponded to *Lagenidium* spp. *cox1*
317 genes, and that the mosquito pathogen *Lagenidium giganteum* is present in phytotelmata (along
318 with *L. humanum*-like isolates). In addition, the sampled sequences, albeit limited in number,
319 validated the newly designed primers as specific for the genus *Lagenidium*. All sequences were
320 incorporated in the phylogenetic analyses described below, in an effort to more precisely
321 determine their taxonomic nature.

322 **Assessment of *Lagenidium* spp. presence in phytotelmata microbiome using *cox1* PacBio**

323 **sequencing:** A total of 40,021 PacBio reads totaling 32,436,900 bp were obtained from one
324 SMRT cell. The average number of full pass per reads was 24.62, and the average read length
325 was 810 bp, matching the amplicons expected lengths. The average quality score per insert was
326 measured at 99.69%. Following the removal of inserts that did not include the mirroring
327 barcodes on both ends (51 reads), a stringent QC threshold was used to eliminate low-quality
328 reads. A total of 23,857 reads were retained, demultiplexed and processed for bioinformatics
329 analyses. Analyzed PacBio sequence datasets (available in the NCBI Sequence Read Archive
330 data under accession numbers SRX6359420- SRX6359423 as part of Bioproject PRJNA550619)
331 included 7,852, 6,576, 5,151 and 4,278 reads for phytotelmata P1 to P4, respectively. Homology
332 searches indicated that only a minority of these filtered reads (227 reads, or 0.9%) could not be
333 assigned a taxonomic classification at the phylum/genus levels. Most sequences were classified

334 into two major eukaryotic phyla, corresponding to animals and protists (Fig. 3). Animal
335 sequences appeared to exclusively belong to insects and related taxa (Fig. 3), consistent with the
336 hypothesis that phytotelmata are actively used environments for a specialized fauna of
337 invertebrates. Protist sequences were further divided into oomycete and non-oomycete
338 subgroups, and, as anticipated, oomycete sequences represented the majority of protist sequences
339 in most sampled communities (Fig. 3). Oomycetes were found especially prevalent in
340 phytotelmata P3 and P4, where they accounted for 79 and 90% of the sequences, respectively.
341 Oomycetes represented 49% of the sequences in the P1 phytotelma, where the sequence
342 distribution was characterized by a large proportion (40%) of invertebrate sequences (Fig. 3).
343 These invertebrate sequences virtually all corresponded to a single OTU closely related to an
344 unidentified Arachnida *coxI* barcode (data not shown). In contrast to the P1, P3 and P4 samples,
345 the P2 filtered reads contained a majority of non-oomycete sequences (Fig. 3), with an
346 overrepresentation (82%) of OTUs homologous to the freshwater diatom genus *Sellaphora* (not
347 shown). Oomycete sequences in P2 represented only 12% of the total sequences generated for
348 this phytotelma (Fig. 3). These results pointed to the promises of using SMRT-based, long read
349 *coxI* sequences to assess the oomycete communities of selected environments but also suggested
350 that the primer sequences, or the amplification conditions, used for these analyses may need to
351 be refined in order to limit the production of amplicons from organisms that are phylogenetically
352 close to oomycetes, such as diatoms. Overall, oomycete barcodes were detected in all
353 phytotelmata, and sequence classifications at the genus level revealed a total of 10 oomycete
354 genera, including *Achlya*, *Aphanomyces*, *Halophytophthora*, *Haptoglossa*, *Lagenidium*,
355 *Phytophthora*, *Phytopythium*, *Pythiogeton*, *Pythium* and *Saprolegnia*. As illustrated in Figure 3,
356 *Pythium*, followed by *Lagenidium*, represented the most prevalent genera in the oomycete

357 communities of all phytotelmata. In agreement with the Sanger-based analyses, sequences
358 homologous to *Lagenidium* spp. *cox1* barcodes were detected in all samples. These sequences
359 accounted for 7.2%, 1.7%, 59.8% and 0.3% of all oomycete reads, for phytotelmata P1 to P4,
360 respectively, indicating that *Lagenidium* was present at low frequencies when compared to
361 *Pythium*, except in the case of the P3 sample (Fig. 3). Also in agreement with the Sanger-based
362 analyses, none of the reads identified as *Lagenidium* spp. were identical to the previously
363 published *L. humanum* *cox1* sequence fragment. However, a small number of reads were shown
364 to be 100% homologous to the mosquito pathogen *L. giganteum* *cox 1* gene sequence (accession
365 numbers HQ708210 and KF923742): 3 reads (out of 279) in the P1 sample and 1 read (out of
366 2,345) in the P3 dataset. OTU clustering at 100% distance level recognized identical reads within
367 and between samples, and revealed that a single sequence was consistently the most predominant
368 *Lagenidium* barcode across all four phytotelmata: this predominant sequence was represented by
369 103 reads out of 279 (37%) for P1, 3 reads out of 14 (21%) for P2, 1,215 reads out of 2,435
370 (50%) for P3 and 3 reads out of 13 (23%) for P4. Using a lower distance level for OTU
371 clustering (97%), virtually all PacBio reads clustered with these predominant sequences (not
372 shown), and were associated with the *L. humanum* barcode. Finally, further sequence alignments
373 compared reads obtained through Sanger vs. PacBio technologies. These comparative analyses
374 showed that the overrepresented PacBio reads for P1-P4 were 100% identical to the sequences
375 obtained using Sanger-based technologies for the P3 sample., highlighting the concordance
376 between the two *Lagenidium* spp. barcode detections.

377 **Phylogenetic analyses:** The generation of novel *Lagenidium*-like *cox1* sequences using both
378 traditional and Next-Generation sequencing technologies prompted comprehensive phylogenetic
379 analyses that incorporated these environmental barcodes within a robust alignment of sequences

380 obtained from axenic cultures. The phylogram inferred from Maximum Likelihood analyses
381 (ML) is presented in Fig. 4. The tree was rooted with representatives of the saprolegnian
382 oomycete clade (Fig. 4), and focused on the peronosporalean clade, which includes the well-
383 established *Phytophthora* and *Pythium* genera, as well as the more basal *Albugo* spp. (McCarthy
384 & Fitzpatrick 2017). The tree topology was very consistent with previously published oomycete
385 phylogenies (Beakes et al. 2012; Lara & Belbahri 2011; Spies et al. 2016), and depicted several
386 *Lagenidium* species within a monophyletic clade and as sister taxon to a cluster containing a
387 strongly supported monophyletic grouping of *Phytophthora* spp. and a paraphyletic assemblage
388 of *Pythium* lineages (Fig. 4). The branch leading to *Albugo* spp. remained basal to this
389 *Phytophthora-Pythium-Lagenidium* cluster. Although all *Pythium* species appeared
390 monophyletic, deeper nodes, indicative of relationships between various *Pythium* spp., were
391 characterized by weak statistical support. Similarly, poor bootstrap support prevented the
392 confirmation of a recently proposed *Lagenidium sensu stricto* classification that regrouped *L.*
393 *giganteum*, *L. humanum* and *L. deciduum*, and was inferred from a six-gene phylogeny
394 reconstructions that included *cox1* gene sequences (Spies et al. 2016). However, the present
395 analysis confirmed the strongly supported, monophyletic association between *L. giganteum* and
396 *L. humanum* (Fig. 4). All of the environmental sequences obtained from phytotelmata clustered
397 within this *Lagenidium* clade, strongly validating the metagenomic approach, and the
398 preliminary taxonomic identifications inferred from homology analyses. The environmental
399 barcodes, independently from the amplification strategy and sequencing technology used to
400 obtain them, segregated into two different groups: some sequences, including the most
401 represented sequences generated using NGS technologies, appeared as sister taxa to *L. humanum*
402 (99% bootstrap support), whereas another group of environmental sequences were strongly

403 associated with the *L. giganteum* isolated from mosquito larvae (94% bootstrap support).
404 Interestingly, no sequences appeared close to the *L. giganteum* f. *caninum* clade, or close to the
405 more distant *L. deciduum* (Fig. 4), suggesting that, although the metabarcoding approach used in
406 this study revealed a previously sub-sampled diversity within the genus *Lagenidium*, the
407 sampling strategy may have biased the detection of *Lagenidium* spp. towards species that inhabit
408 very specific ecological niches. The phylogenetic analyses clearly indicated that oomycetes such
409 as *L. giganteum* and (possibly) *L. humanum* are present in phytotelmata, and that the
410 metabarcoding approach described in this study provides a basis for the detection and isolation of
411 novel *Lagenidium* strains independently of host-dependent baiting or occasional observations of
412 infections.

413

414 **DISCUSSION**

415

416 One of the major objectives of this study was to assess the presence of *Lagenidium giganteum* in
417 phytotelmata. Two independent and complementary microbial detection strategies based on the
418 amplification of *cox1* DNA barcodes were used and produced globally concordant outcomes that
419 strongly suggested that *L. giganteum* can colonize small aquatic environments such as
420 phytotelmata, indicating opportunities for close associations not only with invertebrate hosts, but
421 also with plant tissues. The use of a nested PCR strategy that integrated newly designed
422 *Lagenidium*-specific primers generated a majority of sequences that clustered with the previously
423 published *L. giganteum* *cox1* gene fragments (Fig. 4), while high-throughput sequencing using a
424 PacBio platform also produced *cox1* sequences consistent with the presence of *L. giganteum*.
425 Overall, *L. giganteum* DNA barcodes were detected in all 4 sampled phytotelmata (Fig. 4).

426 Furthermore, the two strategies were highly similar in highlighting the presence of potential
427 additional *Lagenidium* species that appeared closer related to *L. humanum*. A single DNA
428 barcode corresponding to a potentially novel *Lagenidium* phylotype was especially prevalent in
429 the high throughput dataset, but was also detected as the only *Lagenidium* sequences in the P3
430 phytotelma by the alternate, nested-PCR-based protocol. Finally, although the sampling size of
431 randomly-selected cloned *cox1* fragments sequenced through Sanger technologies remained
432 modest, both detection methods were remarkable in failing to generate any DNA barcodes that
433 have been associated with *Lagenidium* strains isolated from mammalian hosts. These multiple
434 instances of concordance between methodologies contribute to strengthen the conclusion that
435 specific *Lagenidium* phylotypes, including the entomopathogenic *L. giganteum*, are present in
436 phytotelmata, and validate the use of the PacBio sequencing platforms (combined with *cox1* as
437 DNA barcodes) as a potential strategy to assess oomycete community composition in
438 environments of interest. Especially, the generation of identical Amplicon Sequence Variants
439 (ASVs), with similarly high frequencies among *Lagenidium* spp. barcodes, in four independent
440 plants serves to provide high levels of confidence in the quality of the datasets obtained using the
441 SMRT strategy (Callahan et al. 2017).

442 Comparisons between the two methodologies also revealed some discrepancies, highlighting the
443 limitations of these detection techniques and the opportunity to use early oomycete
444 metabarcoding analyses such as this study to devise more efficient protocols aimed at
445 understanding oomycete communities in taxa-rich, complex substrates. Consistent with previous
446 work (Riit et al. 2016), high throughput sequencing combined with broad range primers resulted
447 in the amplification of non-target barcodes and, in the case of the P2 phytotelma, drastically
448 decreased the sample size of oomycete reads used to assess the presence and relative frequencies

449 of *Lagenidium* spp. (Fig. 3). Although the amplification of barcodes corresponding to microbial
450 fauna representatives that are phylogenetically close to oomycetes (e.g. diatoms) appear difficult
451 to eliminate, the generation of reads associated with animals or fungi suggests that the *cox1*
452 primers, or the amplification conditions, used in this study may be refined to avoid non-target
453 sequencing. Novel primer design sites in the *cox1* or other genes should be investigated to further
454 the demonstrated potential of SMRT-based long-read analyses, and favor the production of DNA
455 barcodes that may prove to be not only longer, but also more oomycete-specific. In addition,
456 combining PacBio sequencing with the use of the presented *Lagenidium*-specific primers and
457 more constricted amplification conditions may offer a more thorough estimate of all *Lagenidium*
458 phylotypes and their respective relative abundance, while limiting the production of DNA
459 barcodes from other oomycetes and non-target organisms. A similar strategy was used
460 previously for the plant pathogenic *Phytophthora*, and demonstrated that next generation
461 sequencing technologies provide higher resolution compared to the traditional cloning/Sanger
462 sequencing approaches, resulting in the detection of a higher number of phylotypes (Prigigallo et
463 al. 2016). However, strategies based on genus specific primers do not offer the opportunity to
464 globally assess oomycete communities. Complementary approaches such as the ones presented
465 in this study are likely necessary to thoroughly appreciate the role and importance of oomycetes
466 such as *Lagenidium* spp. in plant microbiomes and on the invertebrate fauna associated with
467 these environments. Based on this study, the impact on *Lagenidium* spp. on potential invertebrate
468 hosts within phytotelmata remains unclear, as they mostly appeared as low frequency members
469 within oomycete communities, especially relative to *Pythium* (Fig. 3). This observation is
470 consistent with previous metabarcoding analyses of soil oomycetes that demonstrated that
471 Pythiales vastly outnumbered Lageniales (Riit et al. 2016). However, the read distribution

472 obtained from P3 indicates that *Lagenidium* spp. relative frequency may rise under specific (and
473 yet-to-be determined) circumstances, possibly associated with the presence of hosts, or other
474 factors (Fig. 3). Within the genus *Lagenidium*, the relative abundance of multiple distinct
475 phylotypes also remains unresolved: the *Lagenidium*-specific primers produces a majority of
476 sequences that clustered with the *L. giganteum* OTUs (58% vs. 42% clustering with the *L.*
477 *humanum* OTUs), but this observation was not supported by the PacBio sequencing data, which
478 clearly identified *L. humanum* OTUs as the most abundant phylotype, with *L. giganteum*
479 barcodes appearing only marginally (<1%, Fig. 4). It remains unclear if the phylotype
480 distribution obtained through high-throughput sequencing is an accurate representation of the
481 *Lagenidium* spp. community within phytotelmata, or if it only reflects technical artefacts such as
482 primer bias towards particular *cox1* barcodes. As mentioned above, these discrepancies offer the
483 possibility to delineate more clearly-defined protocols for oomycete metagenomics.

484 Beyond the technical aspects, the presented study globally supports the hypothesis that
485 *Lagenidium* spp. are present in phytotelmata and therefore provides novel insights on the
486 ecological niches occupied by these poorly-known oomycetes. Investigating potential
487 relationships with plant tissues within phytotelmata may reconcile the transcriptomics data that
488 have blurred the distinction between plant vs animal pathogens, and identified canonical
489 oomycete effectors in the *Lagenidium* genomes (Quiroz Velasquez et al. 2014). The detection of
490 *Lagenidium* spp. close to plant tissues also provides contextual support for the hypothesis that
491 these oomycetes evolved from plant pathogens, and sheds light on a recurrent evolutionary
492 pathway (shift from plant pathogenicity to entomopathogenicity) that has been observed
493 independently in multiple, phylogenetically unrelated entomopathogens. The most broadly
494 known fungal entomopathogens have been shown to have emerged from plant pathogens and

495 endophytes (St Leger et al. 2011). Recently, a similar transition was proposed for the mosquito
496 pathogenic oomycete *Pythium guiyangense*, indicating that evolution of entomopathogenicity
497 from plant pathogens may have occurred multiple times in oomycete lineages (Shen et al. 2019).
498 Phylogenetic analyses demonstrated that *Py. guiyangense* is nested within *Pythium* clades
499 populated by plant pathogens, suggesting that it evolved pathogenicity to mosquito
500 independently of *Lagenidium giganteum*. Genome sequencing highlighted remarkable
501 convergence between the two mosquito pathogenic oomycetes, including the presence of
502 effectors characteristic of plant pathogens, such as CRN and elicitor proteins (Shen et al. 2019).
503 Overall, data collected on entomopathogenic oomycetes suggest that they have evolved
504 independently from plant pathogens, and have retained similar genes indicative of plant
505 associations. These observations can also be extended to *Py. insidiosum*, which appeared to have
506 shifted from plant pathogenic ancestors and acquired the ability to cause infections in humans
507 and other mammals (Rujirawat et al. 2018). The increasing interest in oomycetes as animal
508 pathogens, and the emerging diversity of oomycete hosts, place a previously unexpected
509 emphasis on developing oomycetes as models for the study of evolution of pathogenic abilities
510 and host selection.

511 Finally, the data generated in this study also highlights the value of culture-independent
512 technologies to appreciate previously-unsampled oomycete diversity within the genus
513 *Lagenidium*, and the potential of bromeliad phytotelmata as a source of novel mosquito
514 biocontrol agents. The consistent generation of novel, similar oomycete DNA barcodes (*L.*
515 *humanum* ASVs) in four independent plants suggests that a yet-to-be characterized *Lagenidium*
516 phylotype may be isolated from phytotelmata, and since it inhabits demonstrated mosquito
517 breeding sites (Wilke et al. 2018), may exhibit potential as vector biocontrol agent. Phylogenetic

518 analyses revealed that this phylotype is more distant from the *L. giganteum* strains responsible
519 for mammal infections, and therefore may prove to present less safety concerns than the *L.*
520 *giganteum* isolates that were originally developed as commercial products, and currently
521 abandoned (Vilela et al. 2019). The phylogenetic affinities exhibited by this potential new
522 *Lagenidium* phylotype also offer the intriguing opportunity to investigate the potential of *L.*
523 *humanum* as an invertebrate pathogen, and biocontrol agent. Despite its species name, *L.*
524 *humanum* has never been reported as a human (or vertebrate) pathogen, but was originally and
525 serendipitously isolated from soil samples using dead human skin pieces as baits (Karling 1947).
526 Its pathogenic abilities remain unknown, and, because of the especially modest publication
527 record focused on this species, it is also unclear if the material available from the ATCC
528 (Specker 1991) corresponds to the original isolate that was thoroughly described and illustrated
529 in 1947 (Karling 1947). Efforts to axenically isolate the major *Lagenidium* phylotype identified
530 in phytotelmata, develop comparative analyses with *L. giganteum* and *L. humanum* strains
531 maintained in culture collections, and evaluate the respective impact of these *Lagenidium* spp. on
532 vector mosquitoes have been initiated.

533 In conclusion, the phylogenetic reconstructions presented in this study were performed primarily
534 to validate the metabarcoding analyses aimed at detecting *Lagenidium giganteum* in
535 phytotelmata. A significant fraction of the DNA barcodes obtained through two independent
536 methods corresponded to *Lagenidium* genes and clustered within a strongly supported,
537 monophyletic clade that included both *L. giganteum* and *L. humanum*. Therefore, *Lagenidium*
538 spp. are members of phytotelmata microbiomes. The development of such validated detection
539 methods may not only be used to assess the prevalence and abundance of *Lagenidium* in relation
540 to invertebrate host presence, but also serves as a basis to investigate potential relationships

541 between *Lagenidium* phylotypes and their plant “host” (especially when invertebrate hosts, and
542 water, are not present), and estimate the role of plant pathogenic-like oomycete effectors during
543 these interactions. Finally, the metabarcoding analyses presented in this study revealed
544 phytotelmata as promising sources for the identification of novel *Lagenidium* strains and/or
545 species with potential as biocontrol agents against vector mosquitoes.

546

547 ACKNOWLEDGEMENTS

548 Support for Next Generation Sequencing technologies was provided by Pacific Biosciences and
549 the University of Florida Interdisciplinary Center for Biotechnology Research (ICBR).

550

551 REFERENCES

552

- 553 Adamowicz SJ. 2015. International Barcode of Life: Evolution of a global research
554 community. *Genome* 58:151-162.
- 555 Beakes GW, Glockling SL, and Sekimoto S. 2012. The evolutionary phylogeny of the
556 oomycete “fungi”. *Protoplasma* 249:3-19.
- 557 Behie SW, and Bidochka MJ. 2014. Ubiquity of insect-derived nitrogen transfer to plants by
558 endophytic insect-pathogenic fungi: an additional branch of the soil nitrogen cycle.
559 *Appl Environ Microbiol* 80:1553-1560.
- 560 Callahan BJ, McMurdie PJ, and Holmes SP. 2017. Exact sequence variants should replace
561 operational taxonomic units in marker-gene data analysis. *The ISME journal*
562 11:2639.
- 563 Cheng T, Xu C, Lei L, Li C, Zhang Y, and Zhou S. 2016. Barcoding the kingdom Plantae: new
564 PCR primers for ITS regions of plants with improved universality and specificity.
565 *Molecular ecology resources* 16:138-149.
- 566 Choi YJ, Beakes G, Glockling S, Kruse J, Nam B, Nigrelli L, Ploch S, Shin HD, Shivas RG, and
567 Telle S. 2015. Towards a universal barcode of oomycetes—a comparison of the *cox1*
568 and *cox2* loci. *Molecular ecology resources* 15:1275-1288.
- 569 Conesa A, Götz S, García-Gómez JM, Terol J, Talón M, and Robles M. 2005. Blast2GO: a
570 universal tool for annotation, visualization and analysis in functional genomics
571 research. *Bioinformatics* 21:3674-3676. 10.1093/bioinformatics/bti610
- 572 Crooks GE, Hon G, Chandonia JM, and Brenner SE. 2004. WebLogo: a sequence logo
573 generator. *Genome Res* 14:1188-1190. 10.1101/gr.849004
- 574 Darriba D, Taboada GL, Doallo R, and Posada D. 2012. jModelTest 2: more models, new
575 heuristics and parallel computing. *Nat Methods* 9:772. 10.1038/nmeth.2109

- 576 Derevnina L, Petre B, Kellner R, Dagdas YF, Sarowar MN, Giannakopoulou A, De la
577 Concepcion JC, Chaparro-Garcia A, Pennington HG, and Van West P. 2016. Emerging
578 oomycete threats to plants and animals. *Philosophical Transactions of the Royal*
579 *Society B: Biological Sciences* 371:20150459.
- 580 Derraik JG. 2009. A tool for sampling mosquito larvae from phytotelmata. *Journal of Vector*
581 *Ecology* 34:155-157.
- 582 Frances S, Sweeney A, and Humber R. 1989. *Crypticola clavulifera* gen. et sp. nov.
583 and *Lagenidium giganteum*: Oomycetes pathogenic for dipterans infesting
584 leaf axils in an Australian rain forest. *Journal of Invertebrate Pathology* 54:103-111.
- 585 Giresse X, Ahmed S, Richard-Cervera S, and Delmotte F. 2010. Development of new
586 oomycete taxon-specific mitochondrial cytochrome b region primers for use in
587 phylogenetic and phylogeographic studies. *Journal of phytopathology* 158:321.
- 588 Guindon S, Dufayard JF, Lefort V, Anisimova M, Hordijk W, and Gascuel O. 2010. New
589 algorithms and methods to estimate maximum-likelihood phylogenies: assessing the
590 performance of PhyML 3.0. *Syst Biol* 59:307-321. 10.1093/sysbio/syq010
- 591 Horner NR, Grenville-Briggs LJ, and van West P. 2012. The oomycete *Pythium oligandrum*
592 expresses putative effectors during mycoparasitism of *Phytophthora infestans* and
593 is amenable to transformation. *Fungal Biol* 116:24-41.
594 10.1016/j.funbio.2011.09.004
- 595 Kamoun S, Furzer O, Jones JD, Judelson HS, Ali GS, Dalio RJ, Roy SG, Schena L, Zambounis A,
596 and Panabières F. 2015. The Top 10 oomycete pathogens in molecular plant
597 pathology. *Molecular Plant Pathology* 16:413-434.
- 598 Karling JS. 1947. *Lagenidium humanum*, a saprophyte isolated on dead human skin.
599 *Mycologia* 39:224-230.
- 600 Kerwin JL, Dritz D, and Washino RK. 1994. Pilot scale production and application in wildlife
601 ponds of *Lagenidium giganteum* (Oomycetes: Lagenidiales). *Journal of the American*
602 *Mosquito Control Association* 10:451-455.
- 603 Kerwin JL, and Petersen EE. 1997. Fungi: oomycetes and chytridiomycetes. In: Lacey L, ed.
604 *Manual of techniques in insect pathology*: Academic Press, 251-268.
- 605 Kress WJ, and Erickson DL. 2007. A two-locus global DNA barcode for land plants: the
606 coding rbcL gene complements the non-coding trnH-psbA spacer region. *PLoS one*
607 2:e508.
- 608 Kress WJ, Wurdack KJ, Zimmer EA, Weigt LA, and Janzen DH. 2005. Use of DNA barcodes to
609 identify flowering plants. *Proceedings of the National Academy of Sciences of the*
610 *United States of America* 102:8369-8374.
- 611 Lara E, and Belbahri L. 2011. SSU rRNA reveals major trends in oomycete evolution. *Fungal*
612 *Diversity* 49:93-100.
- 613 Larkin MA, Blackshields G, Brown NP, Chenna R, McGettigan PA, McWilliam H, Valentin F,
614 Wallace IM, Wilm A, Lopez R, Thompson JD, Gibson TJ, and Higgins DG. 2007. Clustal
615 W and Clustal X version 2.0. *Bioinformatics* 23:2947-2948.
616 10.1093/bioinformatics/btm404
- 617 Lopez DC, and Sword GA. 2015. The endophytic fungal entomopathogens *Beauveria*
618 *bassiana* and *Purpureocillium lilacinum* enhance the growth of cultivated cotton
619 (*Gossypium hirsutum*) and negatively affect survival of the cotton bollworm
620 (*Helicoverpa zea*). *Biological Control* 89:53-60.

- 621 Mancera N, Douma LG, James S, Liu S, Van A, Boucias DG, and Tartar A. 2012. Detection of
622 *Helicosporidium* spp. in metagenomic DNA. *Journal of Invertebrate Pathology*
623 111:13-19.
- 624 McCarthy C, and Fitzpatrick D. 2017. Phylogenomic reconstruction of the oomycete
625 phylogeny derived from 37 genomes. *mSphere* 2: e00095-17. Am Soc Microbiol.
- 626 Mendoza L, Taylor JW, Walker ED, and Vilela R. 2016. Description of three novel
627 *Lagenidium* (Oomycota) species causing infection in mammals. *Revista*
628 *iberoamericana de micologia* 33:83-91.
- 629 Moonjely S, Barelli L, and Bidochka M. 2016. Insect pathogenic fungi as endophytes.
630 *Advances in genetics*: Elsevier, 107-135.
- 631 Nakamura K, Nakamura M, and Hatai K. 1995. *Lagenidium* infection in eggs and larvae of
632 mangrove crab (*Scylla serrata*) produced in Indonesia. *Mycoscience* 36:399-404.
- 633 Olivera IE, Fins KC, Rodriguez SA, Abiff SK, Tartar JL, and Tartar A. 2016. Glycoside
634 hydrolases family 20 (GH20) represent putative virulence factors that are shared by
635 animal pathogenic oomycetes, but are absent in phytopathogens. *BMC Microbiology*.
- 636 Pootakham W, Mhuantong W, Yoocha T, Putchim L, Sonthirod C, Naktang C, Thongtham N,
637 and Tangphatsornruang S. 2017. High resolution profiling of coral-associated
638 bacterial communities using full-length 16S rRNA sequence data from PacBio SMRT
639 sequencing system. *Scientific reports* 7:2774.
- 640 Prigigallo MI, Abdelfattah A, Cacciola SO, Faedda R, Sanzani SM, Cooke DE, and Schena L.
641 2016. Metabarcoding analysis of Phytophthora diversity using genus-specific
642 primers and 454 pyrosequencing. *Phytopathology* 106:305-313.
- 643 Quiroz Velasquez PF, Abiff SK, Fins KC, Conway QB, Salazar NC, Delgado AP, Dawes JK,
644 Douma LG, and Tartar A. 2014. Transcriptome Analysis of the Entomopathogenic
645 Oomycete *Lagenidium giganteum* Reveals Putative Virulence Factors. *Appl Environ*
646 *Microbiol* 80:6427-6436. 10.1128/aem.02060-14.
- 647 Ratnasingham S, and Hebert PD. 2007. BOLD: The Barcode of Life Data System
648 (<http://www.barcodinglife.org>). *Molecular ecology notes* 7:355-364.
- 649 Riit T, Tedersoo L, Drenkhan R, Runno-Paurson E, Kokko H, and Anslan S. 2016. Oomycete-
650 specific ITS primers for identification and metabarcoding. *MycKeys* 14:17.
- 651 Robideau GP, De C, Wam A, Coffey MD, Voglmayr H, Brouwer H, Bala K, Chitty DW,
652 Desaulniers N, and Eggertson QA. 2011. DNA barcoding of oomycetes with
653 cytochrome c oxidase subunit I and internal transcribed spacer. *Molecular ecology*
654 *resources* 11:1002-1011.
- 655 Rujirawat T, Patumcharoenpol P, Lohnoo T, Yingyong W, Kumsang Y, Payattikul P,
656 Tangphatsornruang S, Suriyaphol P, Reamtong O, and Garg G. 2018. Probing the
657 phylogenomics and putative pathogenicity genes of *Pythium insidiosum* by
658 oomycete genome analyses. *Scientific reports* 8:4135.
- 659 Sapkota R, and Nicolaisen M. 2015. An improved high throughput sequencing method for
660 studying oomycete communities. *Journal of microbiological methods* 110:33-39.
- 661 Sasan RK, and Bidochka MJ. 2012. The insect - pathogenic fungus *Metarhizium robertsii*
662 (Clavicipitaceae) is also an endophyte that stimulates plant root development.
663 *American journal of botany* 99:101-107.
- 664 Shen D, Tang Z, Wang C, Wang J, Dong Y, Chen Y, Wei Y, Cheng B, Zhang M, and Grenville-
665 Briggs LJ. 2019. Infection mechanisms and putative effector repertoire of the

- 666 mosquito pathogenic oomycete *Pythium guiyangense* uncovered by genomic
667 analysis. *PLoS Genet* 15:e1008116.
- 668 Singh G, and Prakash S. 2010. Efficacy of *Lagenidium giganteum* (Couch) metabolites for
669 control *Anopheles stephensi* (Liston) a malaria vector. *Malaria Journal* 9:46.
- 670 Specker R. 1991. Lactic acid production by *Lagenidium* spp. *Inoculum (ex Mycol Soc Am*
671 *Newslett)* 42:34.
- 672 Spies CF, Grooters AM, Lévesque CA, Rintoul TL, Redhead SA, Glockling SL, Chen C-y, and De
673 Cock AW. 2016. Molecular phylogeny and taxonomy of *Lagenidium*-like oomycetes
674 pathogenic to mammals. *Fungal Biol* 120:931-947.
- 675 St Leger RJ, Wang C, and Fang W. 2011. New perspectives on insect pathogens. *Fungal*
676 *Biology Reviews* 25:84-88.
- 677 Versieux LM, Barbará T, Wanderley MdGL, Calvente A, Fay MF, and Lexer C. 2012.
678 Molecular phylogenetics of the Brazilian giant bromeliads (Alcantarea,
679 Bromeliaceae): implications for morphological evolution and biogeography.
680 *Molecular Phylogenetics and Evolution* 64:177-189.
- 681 Vilela R, Humber RA, Taylor JW, and Mendoza L. 2019. Phylogenetic and physiological traits
682 of oomycetes originally identified as *Lagenidium giganteum* from fly and mosquito
683 larvae. *Mycologia*:1-15.
- 684 Vilela R, Taylor JW, Walker ED, and Mendoza L. 2015. *Lagenidium giganteum* Pathogenicity
685 in Mammals. *Emerging Infectious Diseases* 21:290-297.
- 686 Wagner J, Coupland P, Browne HP, Lawley TD, Francis SC, and Parkhill J. 2016. Evaluation
687 of PacBio sequencing for full-length bacterial 16S rRNA gene classification. *BMC*
688 *Microbiology* 16:274.
- 689 Wang J, Leger RS, and Wang C. 2016. Advances in genomics of entomopathogenic fungi.
690 *Advances in genetics*: Elsevier, 67-105.
- 691 Wilke AB, Vasquez C, Mauriello PJ, and Beier JC. 2018. Ornamental bromeliads of Miami-
692 Dade County, Florida are important breeding sites for *Aedes aegypti* (Diptera:
693 Culicidae). *Parasites & vectors* 11:283.
- 694

Figure 1(on next page)

Schematic representation of the *cox1* gene as a metabarcoding target

Previously developed, oomycete-specific primers, named OomCox1-LevUp and OomCox1-LevLo, were designed to amplify the 5' end portion of the gene that is typically used as barcode (sometimes referred to as the "Folmer region", especially in metazoans). Oomycete *cox1* sequences obtained using these primers were aligned and evaluated for sites compatible with the development of *Lagenidium* genus-specific primers. As illustrated by the sequence logos, a locus immediately upstream of the OomCox1-LevLo location showed genus-level specificity and was selected for primer design. The logos correspond to the complete primer location (20 bp). Numbers in parentheses indicate the total number of sequences (for each genus) used to generate the logos.

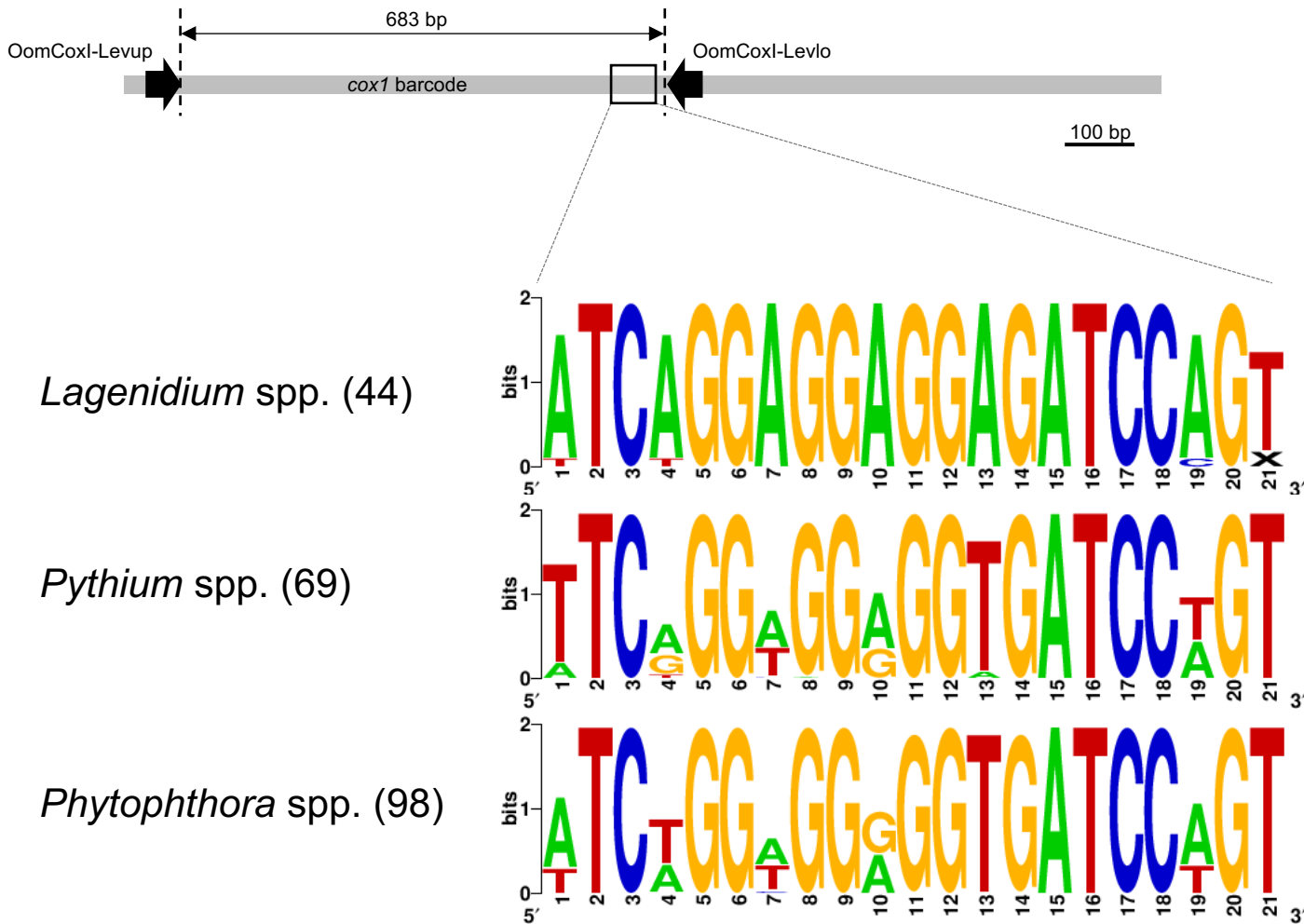


Figure 2(on next page)

Sampled plants and molecular detection of phytotelmata oomycetes

Panels A-D depict the four plants (used as ornamentals on the NSU campus) representing the origin of the phytotelmata samples denoted P1 to P4 throughout the study (plants A-D=phytotelmata P1-P4, respectively). Environmental DNA was extracted from these four plant phytotelmata and tested for the presence of oomycetes using *cox1* primers. Panel E illustrates PCR products generated using these environmental DNA preparations as templates combined with the oomycete-specific *cox1* primers (OomCoxI-LevUp and OomCoxI-LevLo). Phytotelmata metagenomic DNA preparations are labelled as P1-P4, while (+) and (-) lanes represent positive (*L. giganteum* DNA) and negative (no template) control. Additional control reactions (C1, C2) included templates corresponding to metagenomic DNA extracted from water fountain (tap) and ocean waters, respectively. Visible PCR products for lanes P1-P4 demonstrated that oomycetes were readily detected in all sampled phytotelmata.

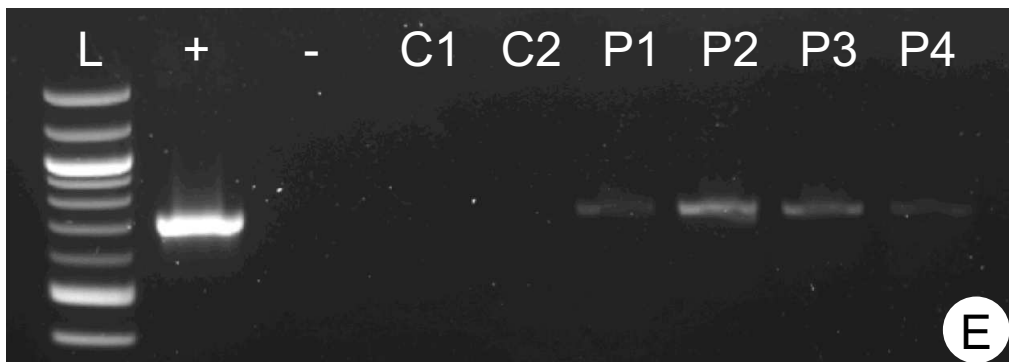
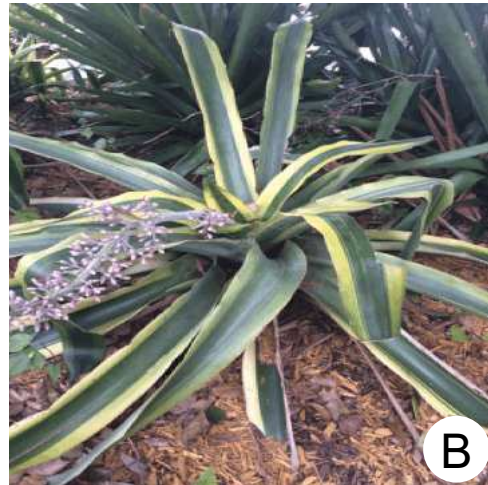
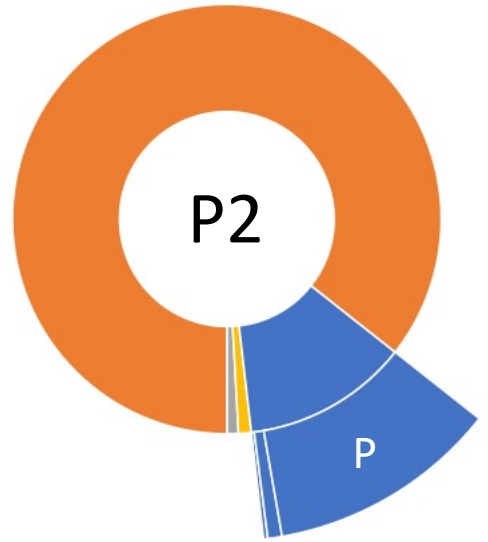
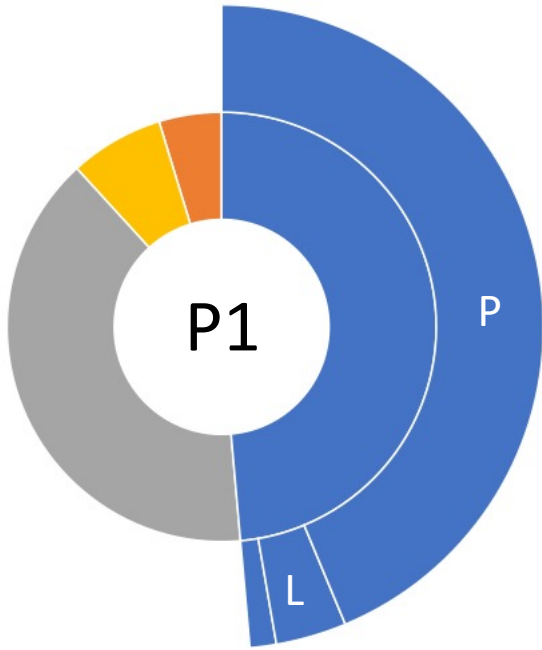


Figure 3(on next page)

Relative taxonomic distribution of *cox1* sequences generated using the PacBio sequencing technology platform

The four sampled phytotelmata are denoted as P1-P4 in the circle centers. As anticipated, the majority of sequences showed similarities to oomycete DNA barcodes (color coded in blue), although sequences corresponding to non-target taxonomic groups were also detected. For oomycetes, a genus-level taxonomic break-down (outer circle portions) demonstrated that the most prevalent genera in phytotelmata were *Pythium* and *Lagenidium*, represented by letters P and L, respectively. All other oomycetes were regrouped into the third classification (i.e. not P nor L). For clarity purposes, letters corresponding to oomycete genera are not indicated when the overall distribution frequency is below 5%.



■ OOMYCETES ■ OTHER PROTISTS ■ INVERTEBRATES ■ OTHERS

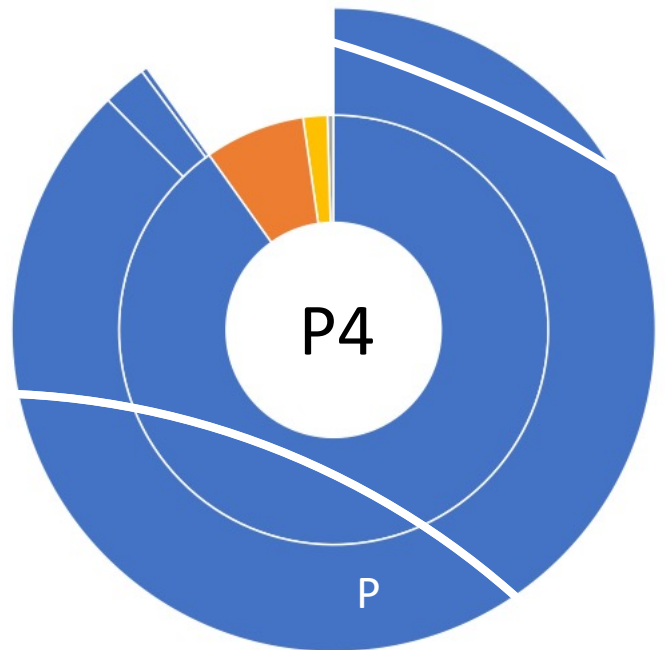
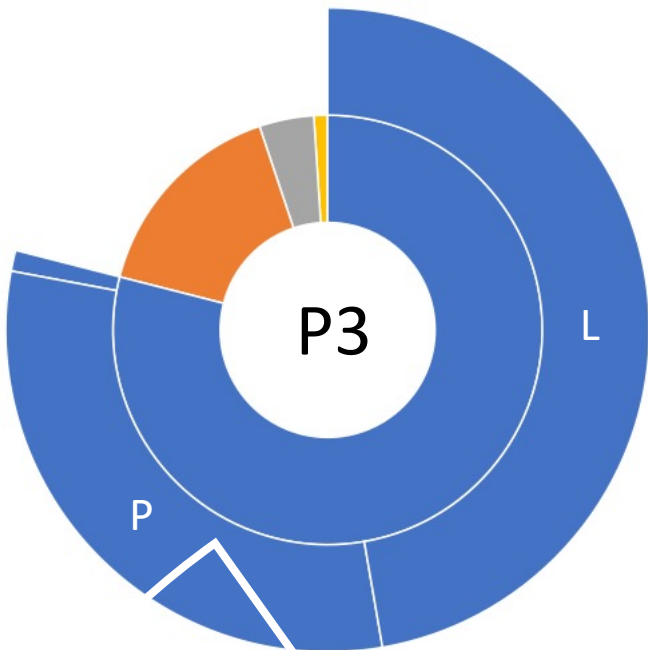


Figure 4(on next page)

Maximum Likelihood (ML) phylogram inferred from oomycete *cox1* gene sequences, and incorporating environmental sequences generated using Sanger or PacBio sequencing strategies.

The origin of these environmental sequences is denoted by the codes P1-P4, corresponding to bromeliad phytotelmata 1 to 4, respectively. All other sequences were downloaded from public databases, except for the *Lagenidium giganteum* ARSEF 373 *cox1* DNA barcode (in bold) which was generated for this study. For environmental sequences, numbers in square brackets indicate the numbers of identical reads obtained throughout the metabarcoding analysis. For non-*Lagenidium* oomycete species, numbers in parentheses indicate the numbers of sequences used to generate the trees. Numbers at the nodes correspond to bootstrap values >50% (1000 replicates), whereas less-supported nodes (<50%) are indicated with (--). The tree is rooted with *Saprolegnia* spp., and demonstrates that *Lagenidium* spp. barcodes were detected in all phytotelmata. All detected *Lagenidium* barcodes clustered within a strongly supported monophyletic clade that include *L. giganteum* and *L. humanum*.

